Microbial community and C cycling across permafrost peatlands in the Hudson Bay Lowlands: feedbacks to in-situ degradation and simulated warming

by

Adam H. Kirkwood

A thesis submitted in partial fulfillment
of the requirements for the degree of
Masters of Science (M.Sc.) in Biology

The Faculty of Graduate Studies
Laurentian University
Sudbury, Ontario, Canada

THESIS DEFENCE COMMITTEE/COMITÉ DE SOUTENANCE DE THÈSE
Laurentian Université/Université Laurentienne
Faculty of Graduate Studies/Faculté des études supérieures

Title of Thesis Titre de la thèse	Microbial community and C cycling across permafrost peatlands in the Hudson Bay Lowlands: feedbacks to in-situ degradation and simulated warming
Name of Candidate Nom du candidat	Kirkwood, Adam
Degree Diplôme	Master of Science
Department/Program Département/Programme	Biology
Date of Defence Date de la soutenance	November 11, 2019

APPROVED/APPROUVÉ

Thesis Examiners/Examinateurs de thèse:

Dr. Nathan Basiliko
(Supervisor/Directeur de thèse)

Dr. Pascale Roy-Leveillée
(Co-supervisor/Co-directrice de thèse)

Dr. Nadia Mykytczuk
(Committee member/Membre du comité)

Dr. Brian Branfireun
(Committee member/Membre du comité)

Dr. Merrin Macrae
(External Examiner/Examinateur externe)

Approved for the Faculty of Graduate Studies
Approuvé pour la Faculté des études supérieures
Dr. David Lesbarrères
Monsieur David Lesbarrères
Dean, Faculty of Graduate Studies
Doyen, Faculté des études supérieures

ACCESSIBILITY CLAUSE AND PERMISSION TO USE

ABSTRACT

Peatlands in the Hudson Bay Lowlands (HBL) constitute a sensitive and globally significant store of carbon, estimated at approximately 30 Pg, where in the northern portion of the HBL a significant amount of this carbon is stored in permafrost. Particularly, near-surface permafrost in the HBL occurs as palsas which are omnipresent in the HBL. However, permafrost degradation in the HBL is proceeding at an accelerated pace as changing sea-ice dynamics in Hudson Bay amplify the regional effects of climate change. The degradation of permafrost leads to decomposition of organic carbon, which produces two important greenhouse gases; carbon dioxide (CO_2) and methane (CH_4). Under the context of climate change and degrading permafrost conditions in the HBL, this research investigated the microbially mediated production of CO_2 and CH_4 from palsas and adjacent thermokarst features from the Hudson Bay Lowlands, and the effects of palsa evolution on these processes. In August of 2017, cores of active layer, permafrost, and thermokarst were collected from five replicate palsas in the continuous zone of permafrost within a 150 km^2 watershed selected for monitoring by the Ontario Ministry of Natural Resources and Forestry. Short-term aerobic incubations (7 days) at field moisture conditions were used to assess methane production and consumption, and long-term (225 days) anaerobic incubations were used to assess methane production. Peat chemistry was characterized through elemental analysis, including peat substrate chemistry through the use of Fourier-Transform Infrared (FTIR) Spectroscopy. Finally, microbial communities from samples pre- and post-incubation were characterized via Illumina high-throughput sequencing for 16s rRNA. This study finds that active layer samples are capable of oxidizing CH_4 under field conditions, whereas permafrost samples generally produced CH_4.

Under anaerobic conditions, thermokarst samples are much more prolific producers of CH_4 in comparison to permafrost and active layer samples. This study suggests that it is peat chemistry and changes in vegetation associated with the evolution of palsas responsible for increased production of CH_4 from thermokarst. This is the result of combined physical and chemical conditions both conducive to methanogenesis, where differing peat chemistry increases the availability of substrates utilized by methanogens, as well as increased zones of anaerobiosis. This research highlights the need for permafrost carbon models to include degradation of palsas via thermokarst encroachment, as this study demonstrates that it has important implications for the production and release of CH_4.

KEYWORDS:
Permafrost, methane, carbon dioxide, Hudson Bay Lowlands, thermokarst, peat chemistry, methanogens, carbon, palsas and peat plateaus

ACKNOWLEDGEMENTS:
There are many people who made the completion of this M.Sc. thesis possible, that I don't know where to begin. First, I start with my co-supervisors Drs. Pascale Roy-Léveillée and Nathan Basiliko. Pascale – I would like to thank you for helping me 'wake-up' half way though second year geomorphology and taking me under your permafrost wing. You have provided me with countless hours of support and advice both professionally as well as personally, and saw potential in me that I didn't think was possible, and I am incredibly grateful. Nate – I would also like to thank you for the countless hours you've dedicated to helping me grow personally and professionally. You not only want to see me develop academically, but have also shown me that graduate studies isn't just about academic development, but also includes having a personal life and building positive relationships. I truly couldn't have asked for two better supervisors individually, but together is even better. The many thought provoking meetings we've had have pushed me academically, and challenged me to think more critically about research and the questions that need to be answered. Thank you very much to my committee members, and others involved in this project. Thanks to Drs. Nadia Mykytczuk, Maara Packalen, and Jim McLaughlin for all of the help on so many different aspects of this project, and pushing me to write the best possible thesis I could.

I would like to thank everyone that is at the Vale Living with Lakes Centre. Working here is truly incredible, and working with other students and faculty both within and outside of my field has been incredibly useful. Conversations around the lunch table have ranged from goofy topics we talk about to kill time, to enlightening conversations about statistics and data analysis that have pushed this project further and further. Special thanks to Emily Smenderovac, who is great at leading the conversations both on goofy topics and statistics, and who without this thesis would have taken me a lot longer.

I also need to dedicate a special paragraph to Karen Oman – Karen, you the real MVP. I am convinced that without you, the Lakes Centre would be chaos, which I can confirm because the weeks you take off it seems that everybody loses their own heads. I look forward to our daily "Hi Karen, Hi Adam" conversations as I frantically look for Pascale in her office to ask her a question I likely could have emailed her. Thank you for everything that you do, and for the incredible organizational skills you possess for keeping us all on track and making sure everyone has everything that they need.

In addition, I would like to thank all of the funding agencies that have made this work possible, especially the W. Garfield Weston Foundation who has supported me financially both for research, and personally. Becoming part of an organization that is dedicated to making positive change is truly honourable. I would also like to thank NSERC for providing funding during this masters.

Finally, I would like to extend my most sincerest of thanks to my family and friends, who have held me up (or more appropriately, picked me up) during the times where everything seemed impossible. Christina, Amy, and Kaylie, thank you for listening to be blab on about frozen ground, and always encouraging me to be my best self.

THESIS FORMAT AND CO-AUTHORSHIP STATEMENT:

This thesis was formatted in such a manner that it will be distilled into a peer-reviewed primary research article that will be submitted to the journal Global Change Biology. I am the primary author of this thesis, however co-authors and committee members contributed in various ways throughout all stages of the thesis:

Dr. Pascale Roy-Léveillée: Assisted conceptual design and field work preparation for collection of permafrost core samples. Aided me with proper laboratory techniques for handling permafrost samples. Assisted with preparation of manuscript through editing.

Dr. Nathan Basiliko: Assisted with conceptual design of the study, and aided with laboratory techniques for gas flux measurements. Contributed to preparation of manuscript through editing.

Dr. Nadia Mykytczuk: Assisted with laboratory component and conceptual design of microbial analysis section of this thesis. Reviewed manuscript and provided comments.

Dr. Maara Packalen: Provided site selection for sampling locations and coordinated field logistics for sampling. Assisted with and coordinated laboratory component for peat chemical analyses. Reviewed manuscript and provided comments.

Dr. Jim McLaughlin: Coordinated field logistics for sampling and assisted with peat chemistry analysis. Reviewed manuscript and provided comments.

Table of Contents

ABSTRACT ..... ***iii***

KEYWORDS: ..... ***iv***

ACKNOWLEDGEMENTS: ..... ***v***

THESIS FORMAT AND CO-AUTHORSHIP STATEMENT: ..... ***vi***

LIST OF TABLES ..... ***viii***

LIST OF FIGURES ..... ***ix***

2. METHODS ***4***

2.1 Field Site Selection **4**

2.2 Field sampling **4**

2.3 Core sub-sampling and microbial greenhouse gas fluxes **5**

2.4 Soil Properties **6**

2.5 DNA Extraction and Amplicon Sequencing **7**

2.6 Data Analysis **8**

3. RESULTS ***10***

3.1 Vegetation **10**

3.2 Greenhouse gas production potential **10**

3.3 Carbon Chemistry **12**

3.4 Microbial Community Structure **13**

3.4.1 Alpha Diversity 13

3.4.2 Beta Diversity 14

4. DISCUSSION ***16***

4.1 Temperature sensitivity of microbial GHG production and oxidation **16**

4.2 Constraints on greenhouse gas production **18**

4.3 Mechanisms of palsa degradation **20**

4.3.1 Shifting vegetation communities 20

4.3.2 Implications for CH_4 oxidation vs. production 22

5. Implications ***23***

6. References ***25***

7. Tables and Figures ***345***

8. Appendix: Supplementary Information ***466***

LIST OF TABLES

Table 1: Vegetation surveys of families in thermokarst fens and palsas. **..... 34**

Table 2: Q_{10} temperature coefficients of CH_4 and CO_2 to a 10˚C for peats from active layer, permafrost, and thermokarst **..... 35**

Table 3: One-way ANOVA for greenhouse gas production and chemical variables measured, by material, site, and depth. **..... 36**

Table 4: Correlation matrix (Pearson's product moment correlation) of CH_4 and CO_2 production in comparison to chemical compounds from FTIR spectroscopy and elemental analysis. **..... 37**

Table 5: Stepwise regression of Shannon diversity to various peat chemical characteristics.**.... 38**

LIST OF FIGURES

Figure 1: Map of the Hudson Bay showing Canadian permafrost distribution, with the HBL outlines in black. Inset B) shows recent (2018) satellite imagery compared to historical air photos of sites likely affected by active layer deepening. Inset C) shows the degradation of a palsa via thermokarst encroachment from recent (2018) satellite imagery compared to historical air photo. **39**

Figure 2: Typical vegetation found on palsas (A) and vegetation typical of thermokarst fens dominated by graminoid PFTs (B) **40**

Figure 3: Production and consumption of CH_4 and CO_2 for anaerobic conditions and field moisture conditions. **41**

Figure 4: Carbon chemistry data as shown by Fourier-Transform Infrared (FTIR) spectroscopy. B-D shows elemental analysis for C:N ratio, Total C, and Total N **42**

Figure 5: Chao1 and Shannon Alpha diversity of 16s rRNA communities pre-incubation (A) and post-incubation (B) **43**

Figure 6: Nonmetric multidimensional scaling ordination of (a) microbial communities pre and post incubation, (b) and of post-incubation microbial communities. Arrows represent chemical properties samples. **44**

Figure 7: Methanogen communities as determined from 16s rRNA for post-incubation and pre-incubation. Communities were scaled to show relative abundance for total samples for each peat type. **45**

1. INTRODUCTION

Northern permafrost soils represent ~16% of the global soil area and store ~50% of the global belowground pool of organic C (Tarnocai et al., 2009). Permafrost peatlands are particularly significant sinks of carbon as decomposition rates are slowed by cold and anoxic conditions (Moore and Basiliko, 2006), resulting in the storage of ~277 Pg of the ~1672 Pg organic C in northern permafrost soils (Schuur et al., 2008). While preserved in frozen ground, this carbon is withdrawn from active biogeochemical cycling. However, climate-induced thaw of permafrost leads to large amounts of previously frozen organic carbon becoming available for microbial decomposition and the production of greenhouse gases such as carbon dioxide (CO_2) and methane (CH_4) (Harden et al. 2012).

An area of particular concern for permafrost degradation is the Hudson Bay Lowlands (HBL) (Fig. 1), the largest peatland in North America, and the second largest continuous peatland in the world. The HBL extends from the western coast of Hudson Bay to the eastern coast of James Bay, covering an area of ~372,000 km^2 (Riley, 2011). The HBL emerged from the Tyrell Sea following the retreat of the Laurentide ice sheet, ~8,500 cal yr BP, and is still uplifting at rates of ~10 mm/year, among the fastest globally (Andrews et al., 1983; Sella et al., 2007). The resulting extensive low-grade terrain, in conjunction with saturated environments and a cool climate, allowed for rapid peatland initiation and development over the glaciomarine deposits, leading to the storage of approximately 30 Pg of organic C (Glaser et al., 2004; Packalen et al., 2014). Despite the low latitude, the HBL hosts a sub-arctic climate due to the cooling effect of sea ice persisting in spring and early summer on Hudson and James Bay (Gough et al., 2004), resulting in the lowest latitude continuous permafrost in North America (Figure 1).

Palsas and peat plateaus are common permafrost features along the continuous-discontinuous zone of permafrost (Seppälä, 2011), and are omnipresent in the HBL. Palsas are mounds of frozen peat raised above the surrounding unfrozen wetland by the aggradation of segregated ice layers, and may grow and amalgamate to become peat plateaus (Gurney, 2001). Typically, palsas in the HBL are elevated ~1 m above the surrounding fen, and range in diameter commonly between 10 to 100 m. Palsas and plateaus may experience enhanced degradation through thermokarst encroachment, where heat from surrounding unfrozen wetlands is transferred to the frozen core. This leads to the thaw of permafrost and collapse of the ground surface near the edge of the palsa, which is commonly converted to fen (Dyke and Sladen, 2010; Matthews et al., 1997). Newly formed ponds and wet conditions at the palsa edge contribute to further thermokarst encroachment into the palsa's frozen core. Deepening of the active layer is another mechanism of permafrost degradation that has been shown to affect palsas (Seppälä, 2006), and is widely used in permafrost-carbon feedback assessments (PCF; Burke et al., 2013).

Permafrost environments, such as palsa fields in the HBL, have spatially heterogeneous moisture conditions, which affect the microbial production of CO_2 and CH_4. Wet conditions, such as those associated with the degradation of icy permafrost, favour increased abundance and activity of methanogens (methanogenic archaea), which are strict anaerobes (Capone and Kiene, 1988). Methane oxidizing bacteria (methanotrophs) convert CH_4 to CO_2 and are most commonly found in aerobic environments, however anaerobic methane oxidation is also of importance (Smemo and Yavitt, 2011). The degradation of permafrost in palsa fields, via thermokarst encroachment or active layer deepening, affects the horizontal and vertical

distribution of aerobic and anaerobic environments and thus affects the balance of methane production and oxidation in these peatlands. In addition to moisture conditions, changes in peat substrate chemistry as a result of permafrost degradation influences microbial production of CH_4 and CO_2 (Hodgkins et al., 2014). The proportion of recalcitrant and labile carbon compounds shifts with permafrost thaw, where increases in easily decomposable labile carbon increases CH_4 production (Hodgkins et al., 2014, Lai 2009).

While past research has shown that palsa fields are degrading in the HBL (Pironkova, 2017), the microbial production of CO_2 and CH_4 from these degrading palsas are unknown, as is the balance between methane production and oxidation. This study elucidated how mechanisms of palsa degradation affect biogeochemical cycling of carbon via microbial production and release of greenhouse gases. In the context of climate change and widespread permafrost degradation across the Hudson Bay Lowlands, the objectives were to (1) determine rates of microbial production and consumption of greenhouse gases from degrading palsas, and assess the temperature sensitivity of these processes; (2) characterize peat soil chemistry and microbial community structure as potential constraints on microbial greenhouse gas production; and (3) postulate how in situ changes associated with mechanisms of palsa degradation may lead to altered GHG production and emissions as a result of changing chemical and biological conditions.

2. METHODS

2.1 Field Site Selection

Sampling sites were located within Polar Bear Provincial Park (PBPP), a remote 24,000 km^2 protected landscape along the Ontario coast of Hudson Bay, located ~600 km north of the nearest year-round road. Samples were collected from five palsas selected by the Ontario Ministry of Natural Resources and Forestry (OMNRF) for long-term monitoring within a 150 km^2 watershed. 10-m resolution SPOT satellite imagery (SPOT Image, Toulouse, France) was used to randomly select replicate palsa sites located 2-10 km from each other (Figure 1). Air photos from 1955 scaled 1:40,000 were accessed through the National Air Photo Library (Ottawa, Canada), and manually compared with recent high-resolution satellite imagery (Microsoft Bing Imagery, 2019) to determine if recent palsa degradation is due to thermokarst expansion. Plant communities in the palsas and surrounding fen environments were surveyed in 1 m^2 quadrats with a visual assessment of dominant plant species and genera (>50% cover by area), moderate (between 10-50% cover), present (<10% cover), or absent.

2.2 Field sampling

At each site, samples of active layer and permafrost were collected on the palsas, and samples of fen material were collected adjacent to portions of palsas that were affected by thermokarst degradation. The active layer was sampled by cutting peat into 10 cm x 10 cm rectangles, varying in depth according to active layer thickness at the site. Since sampling took place in late August, it is assumed that the active layer was near its maximum depth. Permafrost samples were collected using a portable earth drill system (Calmels et al., 2005) and extended to a maximum depth of 91.5 cm. Permafrost cores extended beyond the frozen peat

to the mineral sediment and included segregated ice layers. Fen samples were collected with a 10 x 10 cm box corer, and ranged in length from 37-45 cm. Samples were kept frozen during transport to the laboratory, where they were stored at -20˚C until they were split into 10 cm subsections for processing.

2.3 Core sub-sampling and microbial greenhouse gas fluxes

The core subsections were subsampled to form four identical subsets used to measure the production of CH_4 and CO_2 under anaerobic conditions. Approximately 50 g of material was placed into 250 ml incubation jars sealed with air tight lids fitted with rubber septa to allow for gas sampling. To ensure anaerobic conditions, samples were homogenized and mixed with degassed and deoxygenated water. Oxygen in the jar headspace was removed through four cycles of vacuuming the headspace and filling with O_2-free N_2 gas. For the final cycle, the headspace of N_2 was allowed to equilibrate with atmospheric pressure. Active layer and permafrost samples were also incubated under simulated 'field moisture conditions', meaning that samples were left to thaw undisturbed in the jars, and 25 ppm of CH_4 was added to the headspace to measure the potential for CH_4 oxidation. Thermokarst samples were not included in these field moisture condition incubations since they were entirely saturated and in anaerobic conditions once thawed. Anaerobic samples were incubated for a period of 225 days, whereas field-moisture-condition samples were incubated over a period of seven days. Jars were incubated in growth chambers (BioChambers, Winnipeg, MB, Canada) at 4 and 14˚C. Gasses were sampled by extracting 10 ml of headspace with a syringe, and analyzed through gas chromatography (Greenhouse Gas model, SRI Instruments, Torrance, CA, USA) using a Porapak-Q column (80/100 mesh) maintained at 65˚C to separate gases and a flame ionization

detector with in-line methanizer (reducing CO_2 to CH_4 using a Ni-catalyst) (Godin et al. 2012). A standard gas containing 1000 ppm CO_2 and 10 ppm CH_4 in an air balance (Praxair Inc., Sudbury, ON, Canada), was run every 30 samples for calibration and subsequent calculations of CO_2 and CH_4 concentration (Godin et al., 2012).

2.4 Soil Properties

Subsamples of peat were oven dried at 105˚C for 24 hours, followed by 5 hours in a muffle furnace at 550˚C with weighing at each step to measure moisture content and estimate organic matter content. For further chemical analysis, subsamples were freeze-dried for 24 hours and ground with a Wiley Mill (Thomas Scientific, Swedesboro, NJ, USA) with a 1x1mm mesh screen. Total elemental carbon and nitrogen was assessed with an Elementar Vario Max C and N analyzer (Elementar Analysensysteme, Hanau, Germany) (Myers et al., 2012). Carbon structure from peat samples was evaluated using Fourier transform infrared (FTIR) spectroscopy on a Bruker Tensor 27 FTIR spectrometer (Bruker Instruments, Billerica, MA, United States) fitted with a KBr beam splitter (Haynes et al., 2015). Scans of absorbance every 4 cm^{-1} were taken between the range of 500-4000 cm^{-1} wavelengths. The ratios of wavenumbers associated with carboxylic acids (1720 cm^{-1}), aromatic groups (1630 cm^{-1}), and lignins (1515 cm^{-1}; Niemeyer, Chen, and Bollag 1992; Cocozza et al. 2003) were calculated in respect to polysaccharides (1030 cm^{-1}) to calculate “humification indices” (Hodgkins et al., 2014) as a proxy for the level of decomposition in the samples.

2.5 DNA Extraction and Amplicon Sequencing

DNA was extracted from each 10 cm subsection of the active layer, permafrost, and thermokarst cores before they were incubated, and again after 225 days of anaerobic incubation. Small subsamples were taken from frozen cores and kept frozen until immediately before DNA extraction. After 225 days of incubation, samples in the incubation jars were homogenized, and subsampled for immediate DNA extraction. DNA was extracted using a Qiagen DNeasy Power Soil Kit (Qiagen, Germantown, MD, USA) following manufacturer's protocol. DNA was eluted to a final volume of 100 µL in the C6 solution from the DNeasy Power Soil Kit. The extracted DNA was subsequently assessed with absorbance methods using a Take3 Spectrophotometer on a Synergy HI microplate reader (BioTek, Winooski, VT, United States). Extracted DNA was sent to Metagenome Bio Inc. (Toronto, Canada) for sequencing on the Illumina MiSeq platform (Illumina Biotechnology CO., San Diego, CA, United States). Following the methods of Yakimovich et al., (2018), we targeted the V3-V4 regions of bacterial 16S rRNA genes using primers 515FB (5'-GTG YCA GCM GCC GCG GTA A-3') and 806RB (5'-GGA CTA CNV GGG TWT CTA AT-3') (Walters et al., 2016). For sequencing, primers contained Illumina adaptor sequences and priming sites. PCR reactions were done in triplicate to reduce PCR bias, and were 25 µl in total, including 1-10 ng DNA, 5 µl of standard OneTaq buffer (5x), 0.25 µl of 25 mM dNTP, 0.5 µl of forward and reverse primers (10 µM each), 1 µl BSA (12 mg/ml), 0.125 µl of OneTaq DNA polymerase (NEB), and water up to 25 µl. PCR reactions began at 94˚C for 5 min, followed by 30 cycles of denaturing at 94˚C for 30 sec, annealing at 45˚C for 45 sec, and extension at 68˚C for 1 min, and finished with 68˚C for 10 min. PCR products were checked on 2% agarose gels, and DNA was excised and isolated with a Qiagen MinElute gel extraction kit

(Qiagen, Hilden, Germany). The purified library DNA was quantified using a Qubit dsDNA HS assay kit (Life Technologies, CA, United States), and the library pool was spiked with 5% phiX control (V3, Illumina) to improve base imbalance. Finally, paired-end sequencing with read lengths of 251 bp was performed using a MiSeq Reagent Kit V2 (2 x 250 cycles) on an Illumina MiSeq sequencing system.

2.6 Data Analysis

Illumina sequence data were processed with the DADA2 pipeline (Callahan et al., 2016) following package guidelines. Samples were filtered to remove ambiguous base pairs, remove phiX control to prevent misclustering, and to remove sequences with high estimated errors. After quality filtering, both forward and reverse reads were truncated to 180 bp. For forward and reverse reads, the sample inference algorithm was applied to the dereplicated data to determine how many reads occur in how many unique amplicon sequence variants (ASVs) per sample. Forward and reverse reads were merged with overlap set to 12 bp with zero tolerance for mismatching basepairs in the overlap region. Next, chimeras were removed and sequence tables were constructed for taxonomic assignment using the Silva version 132 database (Callahan, 2018) with DADA2's naïve Bayesian classifier method. Taxonomic data were then exported and used in R with the Phyloseq package for downstream analysis (McMurdie and Holmes, 2013; R Core Team, 2018).

Alpha diversity was calculated using the estimate richness function in phyloseq for Chao1 and Shannon diversity measures. Diversity was calculated before filtering any taxonomic data, since richness estimates are highly dependent on the number of singletons in the dataset (McMurdie and Holmes, 2013). One-way analysis of variance (ANOVA) were used to assess

variation of ASV richness between peat types, pre- vs. post-incubation, and site. Post-hoc comparisons using Tukey's Honest Significant Difference (HSD) were used if ANOVAs revealed significant variations (Horton et al., 2019). To determine how peat chemistry affected microbial communities, richness estimates were correlated to peat chemistry using Pearson's product moment correlations. A backward stepwise regression using the MASS package in R (Venables and Ripley, 2002) was used to distinguish how peat chemistry influences diversity and subsequently GHG production.. For beta diversity analysis, abundance data were normalized using the DeSeq2 package in R (Love et al., 2014), including variance stabilizing transformation to address the size of DNA sequencing libraries, as well as ASV count proportions (Horton et al., 2019; McMurdie and Holmes, 2014). These data were then used to examine how the structure of microbial communities changed amongst peat types, site, and with other variables.

Bray-Curtis dissimilarity was calculated and used to show dissimilarity in microbial community structure, visualized using a non-metric multidimensional scaling (NMDS) plot. Using the envfit function of the Vegan package in R (Oksanen et al., 2019), we correlated microbial community structure based on the NMDS plot with peat chemistry data following the methods of Horton et al., (2019). Permutational Multivariate Analysis of Variance (PerMANOVA) using the ADONIS function in vegan was used to analyze how microbial community structure differed by peat type, pre- vs. post-incubation, incubation temperature, and site. To assess community structure of methanogens, sequences of methanogens were subset into a new dataframe and used for downstream analysis. Methanogen community structure, CH_4 and CO_2 production, alpha diversity and peat chemistry data were all plotted using ggplot2 (Wickham, 2016). CH_4 and CO_2 were correlated to environmental variables (peat

type, site, temperature) as well as to peat chemistry data using one-way ANOVAs or Pearson Correlations, where appropriate.

3. RESULTS

3.1 Vegetation

Vegetation on the palsas primarily consisted of hummock forming species *Sphagnum fuscum* and *Sphagnum capillifolium*, as well as various species of lichens (Figure 2a; Table 1). Palsas were surrounded by fens, including areas where air photo analysis indicated that palsas and peat plateaus had degraded via thermokarst (Figure 1b). Since these thermokarst areas were indistinguishable from the surrounding fen, and since all fen samples were collected near palsas, the fen areas sampled for this research were assumed to be thermokarst fens. These fens were dominated by sedge lawns, including cottongrass tussocks (*Eriophorum vaginatum*), and dwarf birch (*Betula nana;* Figure 2b). Selected palsas were ~1 m above the surrounding fen, and were thus raised above the water table, whereas water table was at the surface in the fens.

3.2 Greenhouse gas production potential

After 225 days of anaerobic incubation at 4˚C, there were significant differences ($p<0.001$) in production of CH_4 and CO_2 between peats from the active layer, permafrost, and thermokarst fen samples. Throughout the incubation, active layer and permafrost samples produced small amounts of CH_4, with no significant difference between the two peat types ($p = 0.67$). However, thermokarst produced a much larger amount of CH_4 ($p < 0.001$) than both active layer and permafrost: ~7x more CH_4 than permafrost, and ~90x the amount produced in the active layer (Figure 3a). Production of CO_2 was also highest in thermokarst ($p < 0.001$),

though the differences were not as large as seen for CH_4 (Figure 3b). Thermokarst produced 1.5x more CO_2 than the active layer and 2x more than permafrost and there was a significant difference in CO_2 production between the active layer and permafrost ($p = 0.003$), where the active layer produced larger amounts of CO_2.

Under field-moisture-condition incubation at 4˚C (permafrost and active layer samples only), a considerable amount of CH_4 was oxidized within the first day in the active layer and permafrost samples, however production increased over time and there was net CH_4 production by the seventh day of incubation (Figure 3c). Although general patterns of net flux looked similar over the incubation period (Figure 3c), there was significantly higher net CH_4 production in the permafrost than in the active layer at day 7 ($p<0.001$). CO_2 production increased consistently throughout the incubation, with no significant difference in production between active layer and permafrost ($p = 0.26$; Figure 3d). Field-moisture-condition incubations at 14˚C showed that less CH_4 was oxidized initially (after 1 day) compared to at 4˚C, but overall there was a total decrease in CH_4 concentration over the 7 day incubation (Figure 3e). Similar to incubation at 4˚C, there was a significant difference between CH_4 flux in active layer and permafrost ($p<0.001$), with permafrost having higher concentrations remaining in the incubation jars at day 7. By the end of the incubation, there was no significant difference in CO_2 production between the two peat types (Figure 3f).

Temperature of the incubation was an important control on both CH_4 and CO_2 for anaerobic and field-moisture-condition incubations ($p<0.01$). Q_{10} values for CH_4 were lower under field-moisture-conditions, meaning microbial CH_4 cycling is less sensitive to increased temperature relative to under strictly anaerobic conditions. Under both incubation conditions

and for peat from all landforms, CO_2 production doubled when the temperature was increased by 10˚C, with Q_{10} values consistently around two (Table 2). Under anaerobic conditions, CH_4 production from active layer peat was extremely sensitive to temperature (Q_{10} = 95.5), followed by permafrost peat (Q_{10} = 25.3), and finally thermokarst peats (Q_{10} = 6.4). Q_{10} values increased with increasing depth in the soil profile ($r = 0.36$, $p < 0.001$). Q_{10} values were also correlated with the relative abundance of the purportedly less bioavailable carbon compounds lignins ($r = 0.23$, $p < 0.001$), and aromatics ($r = 0.15$, $p = 0.02$).

3.3 Carbon Chemistry

Humification indices from FTIR spectra showed that permafrost peat generally has the lowest relative amount of recalcitrant carbon compounds (Figure 4a). Active layer and thermokarst generally had greater humification indices, which implies that there was greater prevalence of recalcitrant carbon compounds in these peat types. Ratios of aromatic and lignin compounds did not significantly differ between the three peat types, but carboxylic acids were highest in the active layer compared to permafrost and thermokarst peats (Table 3, Tukey's: AL-PF $p = 0.003$, AL-TKST $p = 0.001$, PF-TKST $p = 0.98$).

Regarding GHG production, CO_2 was more strongly linked to the chemical composition of the peat compared to CH_4. CO_2 production rates correlated with each suite of carbon compounds detectable with our FTIR-spectroscopy method (Table 4), however not with pH. Conversely, pH was a significant ($r = 0.27$, $p = 0.049$) predictor of CH_4 production, where higher pH from thermokarst samples had higher CH_4 production. Lignins, aromatic compounds, and total N were also moderately strong predictors of CH_4 production, all of which were also higher in abundance in thermokarst peat samples (Table 4; Figure 4). Carbon to nitrogen ratios and

total N did not differ between the three peat types (Figure 4 b,d). Contrastingly, there were significant differences in total C, with highest concentrations in the active layer, followed by thermokarst and finally permafrost (Figure 4c; $p = 0.041$). Total C was not a significant predictor of CH_4 production ($r = 0.22$, $p = 0.12$), indicating that CH_4 production is likely controlled by the availability of very specific substrates that were not measured in this study (H_2, CH_3COOH, etc.) rather than overall carbon content. However total C was a significant predictor of CO_2 production ($r = 0.50$, $p < 0.001$).

3.4 Microbial Community Structure

3.4.1 Alpha Diversity

After Illumina Mi-Seq 16s rRNA gene sequencing, there was a total of 4,078,284 sequences across the 162 soil samples. After filtering, denoising, merging, and chimera removal, a total of 3,178,478 sequences remained forming 13,915 amplicon sequence variants (ASVs). In pre-incubation samples, mean Chao1 diversity was highest in permafrost samples and lowest in active layer samples (Figure 5a; ANOVA; $F = 7.325$, $p = 0.001$). When evenness of ASVs present was taken into account with Shannon diversity, thermokarst then had the highest mean diversity, followed by active layer and finally permafrost ($F = 10.83$, $p < 0.001$; Figure 5a). Following 225 days of incubation, Chao1 diversity shifted to where mean diversity was highest in thermokarst, and lowest in active layer (Figure 5b). (ANOVA; $F = 7.06$, $p = 0.001$). Chao1 diversity increased after incubation at 14˚C. Post incubation Chao1 diversity was greater at 14 ˚C than 4˚C (Tukey's: $p = 0.003$ and $p = 0.005$, respectively). Shannon diversity was slightly higher after incubation than pre-incubation ($p = 0.09$), but followed the same pattern as pre-incubation where diversity was highest in thermokarst samples.

Interestingly, Chao1 is not correlated with CH_4 or CO_2 production, whereas Shannon diversity is significantly moderately correlated with both ($r = 0.27$, $p = 0.006$ and $r = 0.28$, $p = 0.005$, respectively). Backward stepwise regression analysis indicated that several elements and compounds control Shannon diversity, and these likely affect CH_4 production (Table 5). Only a few elements and compounds were found to be insignificant in the model and were removed, including polysaccharides, Total N, and S, despite these being individually correlated with Shannon diversity (Supplementary Table 1). Lignins and total N were positively correlated with Shannon diversity ($r = 0.38$, $p = 0.004$ and $r = 0.31$, $p = 0.03$, respectively). The high abundance of lignin and total N in thermokarst samples (Figure 4), coupled with high Shannon diversity (Figure 5) indicated that these are important factors affecting microbial communities.

3.4.2 Beta Diversity

After filtering for dominant ASVs, 211 taxa remained for beta diversity analysis. Microbial communities slightly differed based on peat type (PerMANOVA; $R^2 = 0.16$, $p < 0.001$). In permafrost and thermokarst samples, Proteobacteria were dominant in the majority of the samples, followed by Bacteroidetes. In the active layer, Acidobacteria were more common in comparison to permafrost and thermokarst, and also had a higher presence of Verrucomicrobia and the phylum WPS-2. There were no large shifts in dominant community structure between samples incubated at 4˚C versus those incubated at 14˚C (PerMANOVA; $R^2 = 0.013$, $p = 0.07$), nor were there shifts from pre- to post-incubation (PerMANOVA; $R^2 = 0.02$, $p < 0.001$; Figure 6a).

NMDS ordination showed that there were separations between microbial communities based on peat type (Figure 6b), with active layer, permafrost, and thermokarst grouped as individuals on the ordination. Separation of the active layer was the most clearly defined,

whereas the split between thermokarst and permafrost was less clear. Carbon chemistry correlates well with microbial community structure according to the NMDS plot. The separation between active layer and thermokarst included differences in abundance of carboxylic acids, aliphatics, aromatics, total C and total N, and lignin. Active layer and permafrost communities had differing C:N ratio, as well as concentration of polysaccharides in the samples. Less clear was the split between permafrost and thermokarst, where pH is the only variable significant between the two peat types (Figure 6b).

Of the complete 16s rRNA sequence data (pre and post incubation), Archaeal reads comprised <1% of the total data. After sub-setting for only sequences of Archaea, sequences associated with methanogens were responsible for ~47% of the dataset. In general, samples were dominated by families *Methanobacteriaceae* and Rice Cluster II (RC-II), both of which utilize the hydrogenotrophic pathway (H_2/CO_2 reduction) for methanogenesis (Figure 7). Before incubation, RC-II was dominant in the active layer, responsible for ~50% of methanogen sequences. In permafrost and thermokarst, RC-II was still abundant, but less so than in the active layer. Pre-incubation, permafrost had a higher diversity of methanogen families in comparison to active layer and thermokarst, with *Methanosarcinaceae*, *Methanosaetaceae* and *Methanoperedenaceae*. All but the latter family were also present in thermokarst, and only *Methanosaetaceae* was found in the active layer in addition to *Methanobacteriaceae* and RC-II. Thermokarst samples had a higher abundance of *Methanosaetaceae*, which utilize the acetoclastic pathway to break down a molecule of acetate (CH_3COOOH) to produce CH_4 and CO_2 (Figure 7b). Post-incubation, the structure of methanogens is similar to pre-incubation, except that *Methanobacteriaceae* were more successful than RC-II, especially in permafrost

samples. *Methanoregulaceae* which is also a hydrogenotrophic methanogen, increased in abundance post-incubation for active layer and thermokarst (Figure 7a). This shift in community structure indicated that as permafrost thaws, dominant methanogen communities in the active layer and permafrost favoured a hydrogenotrophic metabolism, whereas acetoclastic methanogens remain abundant in thermokarst.

4. DISCUSSION

4.1 Temperature sensitivity of microbial GHG production and oxidation

Considerable differences in temperature sensitivity of CH_4 and CO_2 production between the three peat types were observed during anaerobic incubations. Gas production was most sensitive to increased temperatures in active layer samples, and least in samples from thermokarst fens. CH_4 fluxes in the field-moisture condition incubations were also sensitive to temperature (Figure 3). At 14˚C, in particular, there was immediate net production of CH_4 from permafrost samples, with an average Q_{10} of 2.1, but sustained net oxidation throughout the 7 days of incubation from active layer samples, with a Q_{10} value of 0.7. Field-moisture condition Q_{10} values were comparable to other studies, where CH_4 production and oxidation commonly have Q_{10} values between 0.6 to 2.9 (Lau et al., 2015; Whalen, 2005). A Q_{10} below 1 indicates an inverse thermal dependence of net efflux, where CH_4 concentrations decreased in incubation jars with increased temperature due to proportionally increased CH_4 oxidation by methanotrophs. Generally, methanotrophy can occur at a broader range of temperatures (Le Mer and Roger, 2001), and these results suggest that, as temperature increases, the potential for CH_4 oxidation is greater than CH_4 production in the active layer.

Previous studies suggest that variations in temperature sensitivity for CH_4 production may be due to differences in the quality of organic material being decomposed, as well as the function and composition of microbial communities (Heslop et al., 2019). Our results support that peat chemistry influences temperature sensitivity, since Q_{10} values were positively correlated to broad groups of recalcitrant aromatic carbon polymers, including lignins. A larger abundance of recalcitrant compounds confers greater activation energy required to begin oxidative decomposition, therefore increasing temperature sensitivity (Davidson and Janssens, 2006; Lupascu et al., 2012). The concentration of lignins was lower in active layer and permafrost samples (Figure 4a), which is not consistent with this explanation, but there may have been other groups of recalcitrant compounds affecting temperature sensitivity in the active layer, perhaps in association with the Sphagnum moss cover on palsas in contrast to the sedge dominated peats from thermokarst fens (Verhoeven and Toth, 1995).

It is unlikely that differences in microbial community structure were responsible for the high temperature sensitivity observed, since the communities were very similar between samples incubated at 4˚C and those incubated at 14˚C. However, the activity rates of microbial communities may be affected by increased temperature, subsequently increasing soil respiration rates (Davidson and Janssens, 2006). At higher temperatures the activity rates of methanogens increases (Zinder, 1993). Increased activity rates may be supported by the increased production of substrates necessary for methanogenesis by other guilds of microbes such as groups of fermenters or H_2 producing bacteria (Conrad et al., 1987). In our samples we see a shift to a predominantly hydrogenotrophic metabolism in active layer and permafrost from pre- to post-incubation, which is in line with other studies suggesting that this shift occurs

with warmer temperatures (Figure 7) (Conrad et al., 1987; Horn et al., 2003). In association with this shift, increased rates of hydrogenotrophic methanogenesis and associated H_2 consumption reduce product-concentration-limitations by the methanogen syntrophs and allows for increased production of H_2 (Worm et al., 2010). This feedback may have contributed to the observed increased CH_4 emissions at higher temperatures.

4.2 Constraints on greenhouse gas production

4.2.1 Carbon availability, moisture, and temperature

In thermokarst landscapes, thaw features such as fens, ponds, and lakes interact with local hydrology to create anaerobic zones that are conducive to the production of CH_4 (Schuur et al., 2008). The increased field fluxes of GHGs from thermokarst features in comparison to permafrost features are commonly explained based on environmental conditions such as moisture and temperature, which may influence CH_4 production more strongly than the increased availability of newly thawed permafrost carbon (Cooper et al., 2017; Olefeldt et al. 2013). In this study the high CH_4 production in thermokarst samples was also more than just a function of increased carbon availability, since thawed permafrost samples had comparatively low CH_4 production when incubated under the same temperature and moisture conditions for several months despite being the most labile (Figure 3, Figure 4). However, since this experiment controlled for temperature and wetness, the results presented herein also clearly indicate that other factors controlled the high CH_4 production from thermokarst samples.

The duration of the anaerobic incubations in this study (225 days) is sufficient to allow even slow-growing anaerobic microorganisms to have equal opportunity for growth between the different peat types (Yavitt and Seidman-Zager, 2006). These conditions should thus have

allowed for the establishment of methanogen communities, as O_2 toxicity to methanogens during sampling and incubation preparation is likely to have been reversed by long-term incubations (Yavitt and Seidman-Zager, 2006). In addition, these long incubations would have allowed for the reduction of electron acceptors leading to the support of respiratory processes that are favourable to fermenters and methanogens (Segers, 1998). Despite this, there are still significant differences in community structure and richness between peat types (Figure 5), and significantly higher CH_4 production from thermokarst peat. Therefore, it is suggested that the high CH_4 production observed in thermokarst samples compared to active layer and permafrost is caused by differences in peat substrate quality and microbial community composition.

4.2.2 Vegetation cover, peat chemistry, and microbial community

Several correlations between peat chemistry and microbial diversity provide potential explanation for the large amounts of CH_4 produced by thermokarst. Specifically, thermokarst samples have the highest abundance of total N, and total N is also positively correlated with Shannon diversity. Increased N availability in peatlands results in decreased N limitation for microbial metabolism, for instance via increased phenol oxidase activity, resulting in increased C mineralization as well as the biological production of CH_4 (Bragazza et al 2006).

Methanogen communities were generally dominated by hydrogenotrophic methanogens, as represented by Methanobacteriaceae and RC-II taxa being the most abundant from each peat type (>50%; Figure 7). This is consistent with other studies that find H_2 metabolism is the most common route for methanogenesis in peatlands (Horn et al., 2003; Hornibrook et al., 1997; Liebner et al., 2015), although wetlands with higher pH tend to have larger abundances of acetoclastic methanogens (Whiticar et al., 1986). Taxa in active layer and

thermokarst samples support this, where methanogens in the active layer (pH 4.6) belonged to clades using H_2, and in thermokarst (pH 6.4) there are comparatively greater taxa utilizing acetate. One possible explanation for low production of CO_2 and CH_4 from the active layer is provided by Hodgkins et al., (2014), who suggest that low production of these GHGs may be the diversion of decay products into microbial biomass (anabolism) rather than to the production of CH_4 (catabolism). In thermokarst, it is probable that increased supply of acetate fueling acetoclastic methanogenesis was responsible for the increased CH_4 production, as this was the most notable difference in methanogen community between the three peat types (Figure 7). Such increase in abundance of acetate may be the resulting of the conversion of permafrost to thermokarst fens and associated ecological changes such as changes in vegetation (Jorgenson et al., 2001).

4.3 Mechanisms of palsa degradation

4.3.1 Shifting vegetation communities

In a long term study on monitoring changes to palsa fields in Northern Quebec, Laberge and Payette, (1995) found that areas of thermokarst are progressively colonized by sedges and *Sphagnum*. At our sites there was also an increased abundance of sedges from the family *Cyperaceae*, notably *Eriophorum spp.* and *Carex spp.* (Figure 2b, Table 1). The increased abundance of these sedges contributes to altered peat chemistry from that of the *Sphagnum spp.* dominated active layer and permafrost peat (Figure 4). *Carex* sp. and *Eriophorum* sp. supply higher quality C substrates supporting overall faster heterotrophic respiration (Moore and Basiliko 2006) and CH4 production and emissions, the latter also influenced by aerenchyma (Whalen, 2005). Graminoids play an often-reported, but poorly understood link to acetoclastic methanogens over CO_2 reduction pathways (Hines et al., 2008). In thermokarst, the abundance

of sedges increases the amounts of root exudates such as ethanol that are contributed to the system, which can be utilized by acetoclastic methanogens (Galand et al., 2005). In addition to root exudates, a dynamic cycle of thermokarst expansion may have involved warmer temperatures stimulating increased nutrient mineralization and supply that favored vascular plants over Sphagnum mosses (e.g. Dieleman et al., 2015; Larmola et al., 2013). As a result, substrates necessary for acetoclastic methanogenesis are likely provided from the decomposition of these new C inputs (Cooper et al., 2017).

Studies that have amended their incubations with substrates (i.e. H_2/CO_2, glucose, ethanol) necessary for methanogenesis find that the difference in GHG production between peats of different botanical origins decreases significantly (Bergman et al., 2000). Since we did not amend our incubations with any such substrates, this implies that there is a higher abundance of substrates available to methanogens in thermokarst compared to active layer and permafrost. Results from this study are in line with others that show a shift from hydrogenotrophic to acetoclastic metabolism in methanogens along the thaw progression of permafrost (Hodgkins et al., 2014; Liebner et al., 2015). In our study, this shift is also associated with much more prolific rates of CH_4 production from thermokarst samples. Aside from changes in vegetation, transition from permafrost to thermokarst fen also increases the availability of nutrient to microbial communities that assist in the decomposition of organic material (Uhlířová et al., 2007). Together, factors such as changes in vegetation composition, peat chemistry, and availability of nutrients will all contribute to increased CH_4 emissions from thermokarst peat itself.

4.3.2 Implications for CH_4 oxidation vs. production

Whether the dominant pathway of palsa degradation occurs via thermokarst encroachment or active layer deepening has consequences for the production or oxidation of CH_4. Deepening of the active layer results in an anaerobic layer suitable for methanogenesis to occur where the active layer has deepened. However various studies have shown that up to 90% of CH_4 produced can be oxidized through aerobic methanotrophy in the oxic upper portion of the active layer (Frenzel et al., 1992). This study supports this, as a considerable amount of CH_4 was oxidized by active layer samples. This indicates that even though CH_4 production is higher from permafrost samples compared to active layer samples, should palsas and peat plateaus degrade through active layer deepening, the CH_4 produced at the thaw interface and below is likely to be oxidized to CO_2 during diffusion to the surface of the active layer, therefore reducing the net emissions of CH_4 to the atmosphere.

Degradation of palsas through lateral thermokarst encroachment results in increased areas of anaerobic environments that are conducive to methanogenesis. In combination with field conditions (temperature and moisture) that increase the likelihood of CH_4 production (Olefeldt et al., 2013), thermokarst encroachment may shift the CH_4 cycle to net emissions. CH_4 emissions were significantly higher in the top 10 cm of thermokarst, accounting for the majority of CH_4 production (Supplementary Figure 1). Given that the surface peat in thermokarst fen is saturated, aerobic CH_4 oxidation will be restricted, CH_4 production enhanced, and subsequently there will be more CH_4 release to the atmosphere. However, despite a lack of aerobic layer, the potential for CH_4 oxidation may still exist as a result of increased presence of vascular plants in

thermokarst, where plant roots contribute O_2 to anoxic peat necessary for CH_4 oxidation (Watson et al., 1997).

5. Implications

In Canada, it is expected that areas underlain by permafrost will decrease by 16.0-19.7% from the 1990s to the 2090s, and is expected to disappear from most southern margins (Zhang et al., 2008). Though there has been considerable increases in knowledge regarding carbon cycling in permafrost ecosystems, the spatial distribution of carbon release is still not adequately understood (Wagner and Liebner, 2009). Understanding the relationship between mechanisms of palsa degradation and the biogeochemical cycling of carbon is an important contribution to improving how the PCF is portrayed in global climate models. Thus far, models that take into account the PCF approach it from the perspective that permafrost only degrades through active layer deepening (e.g. Burke et al., 2013). Our study indicates that by only taking into account active layer deepening as the primary mechanism of thaw, a considerable amount of CH_4 may be excluded from the model. In fact, Burke et al., (2013) do suggest that thermokarst development is neglected when modelling the PCF. Our research further emphasizes the need that thermokarst encroachment should be taken into account during the modelling process, as it has proven its potential be a significant source of CH_4 to the atmosphere. This research highlights that the way in which palsas and peat plateaus degrade has significant effects on ecological succession and microbial community structure, and the balance between CH_4 production and oxidation. These results are especially important for the Hudson Bay Lowlands, a permafrost peatland of global significance that is expected to experience rapid climate warming (Gagnon and Gough, 2005). As palsa fields and peat plateaus

continue to degrade via thermokarst encroachment as described by Pironkova, (2017), the output of CH_4 to the atmosphere is likely to increase.

6. References

Andrews, J.T., Shilts, W.W., and Miller, G.H. (1983). Multiple deglaciations of the Hudson Bay Lowlands, Canada, since deposition of the Missinaibi (Last-integlacial?) formation. Quaternary Research *19*, 18–37.

Bergman, I., Klarqvist, M., and Nilsson, M. (2000). Seasonal variation in rates of methane production from peat of various botanical origins: effects of temperature and substrate quality. FEMS Microbiology Ecology *33,* 181–189.

Burke, E.J., Jones, C.D., and Koven, C.D. (2013). Estimating the permafrost-carbon climate response in the CMIP5 climate models using a simplified approach. Journal of Climate *26*, 4897–4909.

Callahan, B. (2018). Silva taxonomic training data formatted for DADA2.

Callahan, B., McMurdie, P., Rosen, M., Han, A., Johnson, A., and Holmes, H. (2016). DADA2: High-Resolution sample interference from Illumina amplicon data. Nature Methods *13,* 581–583.

Calmels, F., Gagnon, O., and Allard, M. (2005). A portable earth-drill system for permafrost studies. Permafrost and Periglacial Processes *16*, 311–315.

Capone, D.G., and Kiene, R.P. (1988). Comparison of microbial dynamics in marine and freshwater sediments: Contrasts in anaerobic carbon catabolism1. Limnology and Oceanography *33*, 725–749.

Cocozza, C., D'orazio, V., Miano, T.M., and Shotyk, W. (2003). Characterization of solid and aqueous phases of a peat bog profile using molecular fluorescence spectroscopy, ESR and FT-IR, and comparison with physical properties. Organic Geochemistry *34,* 49–60.

Conrad, R., Schütz, H., and Babbel, M. (1987). Temperature limitation of hydrogen turnover and methanogenesis in anoxic paddy soil. FEMS Microbiology Ecology *3*, 281–289.

Cooper, M.D., Estop-Aragonés, C., Fisher, J.P., Thierry, A., Garnett, M.H., Charman, D.J., Murton, J.B., Phoenix, G.K., Treharne, R., and Kokelj, S.V. (2017). Limited contribution of permafrost carbon to methane release from thawing peatlands. Nature Climate Change *7*, 507.

Davidson, E.A., and Janssens, I.A. (2006). Temperature sensitivity of soil carbon decomposition and feedbacks to climate change. Nature *440*, 165.

Dieleman, C.M., Branfireun, B.A., McLaughlin, J.W., and Lindo, Z. (2015). Climate change drives a shift in peatland ecosystem plant community: implications for ecosystem function and stability. Global Change Biology *21*, 388–395.

Dyke, L.D., and Sladen, W.E. (2010). Permafrost and peatland evolution in the northern Hudson Bay Lowland, Manitoba. Arctic 429–441.

Frenzel, P., Rothfuss, F., and Conrad, R. (1992). Oxygen profiles and methane turnover in a flooded rice microcosm. Biology and Fertility of Soils *14*, 84–89.

Gagnon, A.S., and Gough, W.A. (2005). Trends in the dates of ice freeze-up and breakup over Hudson Bay, Canada. Arctic *56*, 370–382.

Galand, P.E., Fritze, H., Conrad, R., and Yrjälä, K. (2005). Pathways for methanogenesis and diversity of methanogenic archaea in three boreal peatland ecosystems. Applied and Environmental Microbiology *71*, 2195–2198.

Glaser, P.H., Siegel, D.I., Reeve, A.S., Janssens, J.A., and Janecky, D.R. (2004). Tectonic drivers for vegetation patterning and landscape evolution in the Albany River region of the Hudson Bay Lowlands. Journal of Ecology *92*, 1054–1070.

Godin, A., McLaughlin, J.W., Webster, K.L., Packalen, M., and Basiliko, N. (2012). Methane and methanogen community dynamics across a boreal peatland nutrient gradient. Soil Biology and Biochemistry *48*, 96–105.

Gough, W.A., Cornwell, A.R., and Tsuji, L.J. (2004). Trends in seasonal sea ice duration in southwestern Hudson Bay. Arctic 299–305.

Gurney, S.D. (2001). Aspects of the genesis, geomorphology and terminology of palsas: perennial cryogenic mounds. Progress in Physical Geography *25*, 249–260.

Harden, J.W., Koven, C.D., Ping, C.-L., Hugelius, G., McGuire, A.D., Camill, P., Jorgenson, T., Kuhry, P., Michaelson, G.J., and O'Donnell, J.A. (2012). Field information links permafrost carbon to physical vulnerabilities of thawing. Geophysical Research Letters *39*.

Haynes, K.M., Preston, M.D., McLaughlin, J.W., Webster, K., and Basiliko, N. (2015). Dissimilar bacterial and fungal decomposer communities across rich to poor fen peatlands exhibit functional redundancy. Canadian Journal of Soil Science *95*, 219–230.

Heslop, J.K., Walter Anthony, K.M., Grosse, G., Liebner, S., and Winkel, M. (2019). Century-scale time since permafrost thaw affects temperature sensitivity of net methane production in thermokarst-lake and talik sediments. Science of the Total Environment.

Hines, M.E., Duddleston, K.N., Rooney-Varga, J.N., Fields, D., and Chanton, J.P. (2008). Uncoupling of acetate degradation from methane formation in Alaskan wetlands: connections to vegetation distribution. Global Biogeochemical Cycles *22*.

Hodgkins, S.B., Tfaily, M.M., McCalley, C.K., Logan, T.A., Crill, P.M., Saleska, S.R., Rich, V.I., and Chanton, J.P. (2014). Changes in peat chemistry associated with permafrost

thaw increase greenhouse gas production. Proceedings of the National Academy of Sciences *111*, 5819–5824.

Horn, M.A., Matthies, C., Küsel, K., Schramm, A., and Drake, H.L. (2003). Hydrogenotrophic methanogenesis by moderately acid-tolerant methanogens of a methane-emitting acidic peat. Appl. Environ. Microbiol. *69*, 74–83.

Hornibrook, E.R., Longstaffe, F.J., and Fyfe, W.S. (1997). Spatial distribution of microbial methane production pathways in temperate zone wetland soils: stable carbon and hydrogen isotope evidence. Geochimica et Cosmochimica Acta *61*, 745–753.

Horton, D.J., Theis, K.R., Uzarski, D.G., and Learman, D.R. (2019). Microbial community structure and microbial networks correspond to nutrient gradients within coastal wetlands of the Laurentian Great Lakes. FEMS Microbiology Ecology *95*, fiz033.

Jorgenson, M.T., Racine, C.H., Walters, J.C., and Osterkamp, T.E. (2001). Permafrost degradation and ecological changes associated with a warmingclimate in central Alaska. Climatic Change *48*, 551–579.

Laberge, M.-J., and Payette, S. (1995). Long-term monitoring of permafrost change in a palsa peatland in northern Quebec, Canada: 1983–1993. Arctic and Alpine Research *27*, 167–171.

Lai, D. Y. F. "Methane dynamics in northern peatlands: a review." *Pedosphere* 19.4 (2009): 409-421.

Larmola, T., Bubier, J.L., Kobyljanec, C., Basiliko, N., Juutinen, S., Humphreys, E., Preston, M., and Moore, T.R. (2013). Vegetation feedbacks of nutrient addition lead to a weaker carbon sink in an ombrotrophic bog. Global Change Biology *19*, 3729–3739.

Lau, M.C., Stackhouse, B.T., Layton, A.C., Chauhan, A., Vishnivetskaya, T.A., Chourey, K., Ronholm, J., Mykytczuk, N.C.S., Bennett, P.C., and Lamarche-Gagnon, G. (2015). An

active atmospheric methane sink in high Arctic mineral cryosols. The ISME Journal *9*, 1880.

Le Mer, J., and Roger, P. (2001). Production, oxidation, emission and consumption of methane by soils: a review. European Journal of Soil Biology *37*, 25–50.

Liebner, S., Ganzert, L., Kiss, A., Yang, S., Wagner, D., and Svenning, M.M. (2015). Shifts in methanogenic community composition and methane fluxes along the degradation of discontinuous permafrost. Frontiers in Microbiology *6*, 356.

Love, M., Huber, W., and Anders, S. (2014). Moderated estimation of fold change and dispersion for RNA-seq data with DESeq2. Genome Biology *15*, 550.

Lupascu, M., Wadham, J.L., Hornibrook, E.R.C., and Pancost, R.D. (2012). Temperature sensitivity of methane production in the permafrost active layer at Stordalen, Sweden: A comparison with non-permafrost northern wetlands. Arctic, Antarctic, and Alpine Research *44*, 469–482.

Matthews, J.A., Dahl, S.-O., Berrisford, M.S., and Nesje, A. (1997). Cyclic development and thermokarstic degradation of palsas in the mid-alpine zone at Leirpullan, Dovrefjell, southern Norway. Permafrost and Periglacial Processes *8*, 107–122.

McMurdie, P., and Holmes, S. (2013). phyloseq: An R package for reproducible interactive analysis and graphics of microbiome census data. PLoS ONE *8*, e61217.

McMurdie, P.J., and Holmes, S. (2014). Waste not, want not: why rarefying microbiome data is inadmissible. PLoS Computational Biology *10*, e1003531.

Moore, T., and Basiliko, N. (2006). Decomposition in boreal peatlands. In Boreal Peatland Ecosystems, (Springer), pp. 125–143.

Myers, B., Webster, K.L., Mclaughlin, J.W., and Basiliko, N. (2012). Microbial activity across a boreal peatland nutrient gradient: the role of fungi and bacteria. Wetlands Ecology and Management *20*, 77–88.

Niemeyer, J., Chen, Y., and Bollag, J.-M. (1992). Characterization of humic acids, composts, and peat by diffuse reflectance Fourier-transform infrared spectroscopy. Soil Science Society of America Journal *56*, 135–140.

Oksanen, J., Blanchet, F.G., Friendly, M., Kindt, R., Legendre, P., McGlinn, D., Minchin, P.R., O'Hara, R.B., Simpson, G.L., and Solymos, P. (2019). Ordination methods, diversity analysis and other functions for community and vegetation ecologists. vegan: Community Ecology Package.

Olefeldt, D., Turetsky, M.R., Crill, P.M., and McGuire, A.D. (2013). Environmental and physical controls on northern terrestrial methane emissions across permafrost zones. Global Change Biology *19*, 589–603.

Packalen, M.S., Finkelstein, S.A., and McLaughlin, J.W. (2014). Carbon storage and potential methane production in the Hudson Bay Lowlands since mid-Holocene peat initiation. Nature Communications *5*, 4078.

Pironkova, Z. (2017). Mapping Palsa and Peat Plateau Changes in the Hudson Bay Lowlands, Canada, Using Historical Aerial Photography and High-Resolution Satellite Imagery. Canadian Journal of Remote Sensing *43*, 455–467.

R Core Team (2018). R: A Language and Environment for Statistical Computing (R Foundation for Statistical Computing).

Riley, J.L. (2011). Wetlands of the Ontario Hudson Bay Lowland: a regional overview. Nature Conservancy of Canada, Toronto, Ontario, Canada *156*.

Schuur, E.A., Bockheim, J., Canadell, J.G., Euskirchen, E., Field, C.B., Goryachkin, S.V., Hagemann, S., Kuhry, P., Lafleur, P.M., and Lee, H. (2008). Vulnerability of permafrost carbon to climate change: Implications for the global carbon cycle. American Institute of Biological Sciences Bulletin *58*, 701–714.

Segers, R. (1998). Methane production and methane consumption: a review of processes underlying wetland methane fluxes. Biogeochemistry *41*, 23–51.

Sella, G.F., Stein, S., Dixon, T.H., Craymer, M., James, T.S., Mazzotti, S., and Dokka, R.K. (2007). Observation of glacial isostatic adjustment in "stable" North America with GPS. Geophysical Research Letters *34*.

Seppälä, M. (2006). Palsa mires in Finland. The Finnish Environment *23*, 155–162.

Seppälä, M. (2011). Synthesis of studies of palsa formation underlining the importance of local environmental and physical characteristics. Quaternary Research *75*, 366–370.

Smemo, K.A., and Yavitt, J.B. (2011). Anaerobic oxidation of methane: an underappreciated aspect of methane cycling in peatland ecosystems? Biogeosciences *8*, 779–793.

Tarnocai, C., Canadell, J.G., Schuur, E.A., Kuhry, P., Mazhitova, G., and Zimov, S. (2009). Soil organic carbon pools in the northern circumpolar permafrost region. Global Biogeochemical Cycles *23*.

Uhlířová, E., Šantrůčková, H., and Davidov, S.P. (2007). Quality and potential biodegradability of soil organic matter preserved in permafrost of Siberian tussock tundra. Soil Biology and Biochemistry *39*, 1978–1989.

Venables, W.N., and Ripley, B.D. (2002). Modern Applied Statistics with S. Springer *4*.

Verhoeven, J.T.A., and Toth, E. (1995). Decomposition of Carex and Sphagnum litter in fens: effect of litter quality and inhibition by living tissue homogenates. Soil Biology and Biochemistry *27*, 271–275.

Wagner, D., and Liebner, S. (2009). Global warming and carbon dynamics in permafrost soils: methane production and oxidation. In Permafrost Soils, (Springer), pp. 219–236.

Walters, W., Hyde, E.R., Donna Berg-Lyons, Ackermann, G., Humphrey, G., Parada, A., Gilbert, J.A., Jansson, J.K., Caporaso, J.G., and Fuhrman, J.A. (2016). Improved bacterial 16S rRNA gene (V4 and V4-5) and fungal internal transcribed spacer marker gene primers for microbial community surveys. Msystems *1*, e00009–15.

Watson, A., Stephen, K.D., Nedwell, D.B., and Arah, J.R. (1997). Oxidation of methane in peat: kinetics of CH4 and O2 removal and the role of plant roots. Soil Biology and Biochemistry *29*, 1257–1267.

Whalen, S.C. (2005). Biogeochemistry of methane exchange between natural wetlands and the atmosphere. Environmental Engineering Science *22*, 73–94.

Whiticar, M.J., Faber, E., and Schoell, M. (1986). Biogenic methane formation in marine and freshwater environments: CO2 reduction vs. acetate fermentation—isotope evidence. Geochimica et Cosmochimica Acta *50*, 693–709.

Wickham, H. (2016). ggplot2: elegant graphics for data analysis (Springer).

Worm, P., Müller, N., Plugge, C.M., Stams, A.J., and Schink, B. (2010). Syntrophy in methanogenic degradation. In (Endo) Symbiotic Methanogenic Archaea, (Springer), pp. 143–173.

Yakimovich, K.M., Emilson, E.J., Carson, M.A., Tanentzap, A.J., Basiliko, N., and Mykytczuk, N.C.S. (2018). Plant litter type dictates microbial communities responsible for

greenhouse gas production in amended lake sediments. Frontiers in Microbiology *9*, 2662.

Yavitt, J.B., and Seidman-Zager, M. (2006). Methanogenic conditions in northern peat soils. Geomicrobiology Journal *23*, 119–127.

Yavitt, J.B., Basiliko, N., Turetsky, M.R., and Hay, A.G. (2006). Methanogenesis and methanogen diversity in three peatland types of the discontinuous permafrost zone, boreal western continental Canada. Geomicrobiology Journal *23*, 641–651.

Zhang, Y., Chen, W., and Riseborough, D.W. (2008). Transient projections of permafrost distribution in Canada during the 21st century under scenarios of climate change. Global and Planetary Change *60*, 443–456.

Zinder, S.H. (1993). Physiological ecology of methanogens. In Methanogenesis, (Springer), pp. 128–206.

7. Tables and Figures

Table 1: Average abundance of key plant families at thermokarst fens and palsas sites rated as dominant (>50%), abundant (10-50%), present (<10%), or absent.

	Thermokarst Fen	**Palsa**
Cyperaceae (Sedges)	Dominant	Present
Ericaceae (Shrubs)	Present	Abundant
Betulaceae (Dwarf birch)	Present	Present
Pinaceae (Tamarack)	Present	Absent
Salicaceae (Willow)	Abundant	Abundant
Sphagnum	Abundant	Dominant
Lichens	Absent	Dominant

Table 2: Q_{10} temperature coefficients, measuring the sensitivity of CH_4 and CO_2 to a 10˚C increase in incubation temperature for peats from active layer and permafrost for field condition incubations, and for peats from active layer, permafrost, and thermokarst samples for anaerobic incubations

	Field Condition		**Anaerobic**		
	Active Layer	Permafrost	Active Layer	Permafrost	Thermokarst
CO_2	1.9	2.3	1.8	1.9	1.8
CH_4	0.7	2.1	95.5	25.3	6.4

Table 3: Table of results for one-way ANOVA for greenhouse gas production values as well as chemical variables measured, compared by material (active layer, permafrost, and thermokarst), site (5 sites), and depth. Significant differences shown in bold.

	Material		**Site**		**Depth**	
	F-Value	P-Value	F-Value	P-Value	F-Value	P-Value
CH_4	**5.596**	**0.0069**	0.775	0.548	2.459	0.124
CO_2	**4.82**	**0.0129**	1.215	0.319	**14.19**	**<0.001**
Aromatics	1.037	0.363	0.993	0.422	1.025	0.317
Carboxylic acid	**9.715**	**<0.001**	0.812	0.525	**12.04**	**0.00118**
Lignin	2.047	0.141	0.77	0.551	0.074	0.786
Polysaccharides	2.024	0.144	1.2	0.325	2.123	0.152
Carbon (%)	**3.443**	**0.041**	0.868	0.492	**5.809**	**0.0202**
Nitrogen (%)	2.828	0.0702	2.162	0.0904	1.671	0.203
C:N Ratio	0.227	0.798	1.183	0.333	0.06	0.807
pH	**66.41**	**<0.001**	0.87	0.49	**9.891**	**0.00297**
S	**12.94**	**<0.001**	6.885	<0.001	**6.692**	**0.011**
Ca	**45.86**	**<0.001**	3.383	0.011	**87.3**	**<0.001**
K	**50.69**	**<0.001**	1.367	0.248	**74.83**	**<0.001**
Mg	**51.44**	**<0.001**	2.061	0.089	**77.88**	**<0.001**
P	1.42	0.245	3.836	0.005	**0.03**	**0.864**

Table 4: Correlation matrix (Pearson's product moment correlation) of CH_4 and CO_2 production in comparison to chemical compounds from FTIR spectroscopy and elemental analysis. Significant correlations shown in bold.

	CH4		**CO2**	
	r	p	r	p
Polysaccharides	**-0.23**	**0.023**	**-0.48**	**<0.001**
Carboxylic acids	0.04	0.673	**0.31**	**0.002**
Lignins	**0.35**	**0.001**	**0.31**	**0.002**
Aromatics	**0.29**	**0.004**	**0.50**	**<0.001**
Total N	**0.27**	**0.008**	**0.42**	**<0.001**
Total C	**0.20**	**0.050**	**0.49**	**<0.001**
C:N	-0.17	0.094	**-0.29**	**0.005**
pH	**0.23**	**0.026**	-0.09	0.401
S	**0.35**	**0.001**	**0.37**	**<0.001**
Ca	-0.15	0.157	**-0.41**	**<0.001**
K	-0.16	0.121	**-0.41**	**<0.001**
Mg	**-0.20**	**0.049**	**-0.46**	**<0.001**
P	**0.34**	**0.001**	**0.23**	**0.026**

Table 5: Stepwise regression comparing Shannon diversity to various peat characteristics including FTIR peaks and elemental analysis. AIC model selection was utilized with backward progression for individual steps.

Input model: Shannon diversity ~ pH + Polysaccharides + Carboxylics + Lignins + Aromatics + Aliphatics + N + C + C:N + S + Ca + K + Mg + P		
Resolved model: Shannon diversity ~ pH + Carboxylics + Lignins + Aromatics + Aliphatics + C + C:N + Ca + K + Mg + P		
	Estimate	P-Value
Intercept	3.75	<0.001
pH	2.50	0.004
Carboxylic acids	51.46	0.02
Lignins	87.95	<0.001
Aromatics	-72.30	0.003
Aliphatics	-29.55	0.002
Total C	0.048	0.001
C:N	-0.0056	0.002
Ca	-0.000014	0.053
K	0.00056	<0.001
Mg	-0.000077	0.015
P	-0.001	0.0011
Multiple R-squared: 0.2617 Adjusted R-squared: 0.1987 F-statistic: 4.157 on 11 and 129 DF, p-value <0.001		

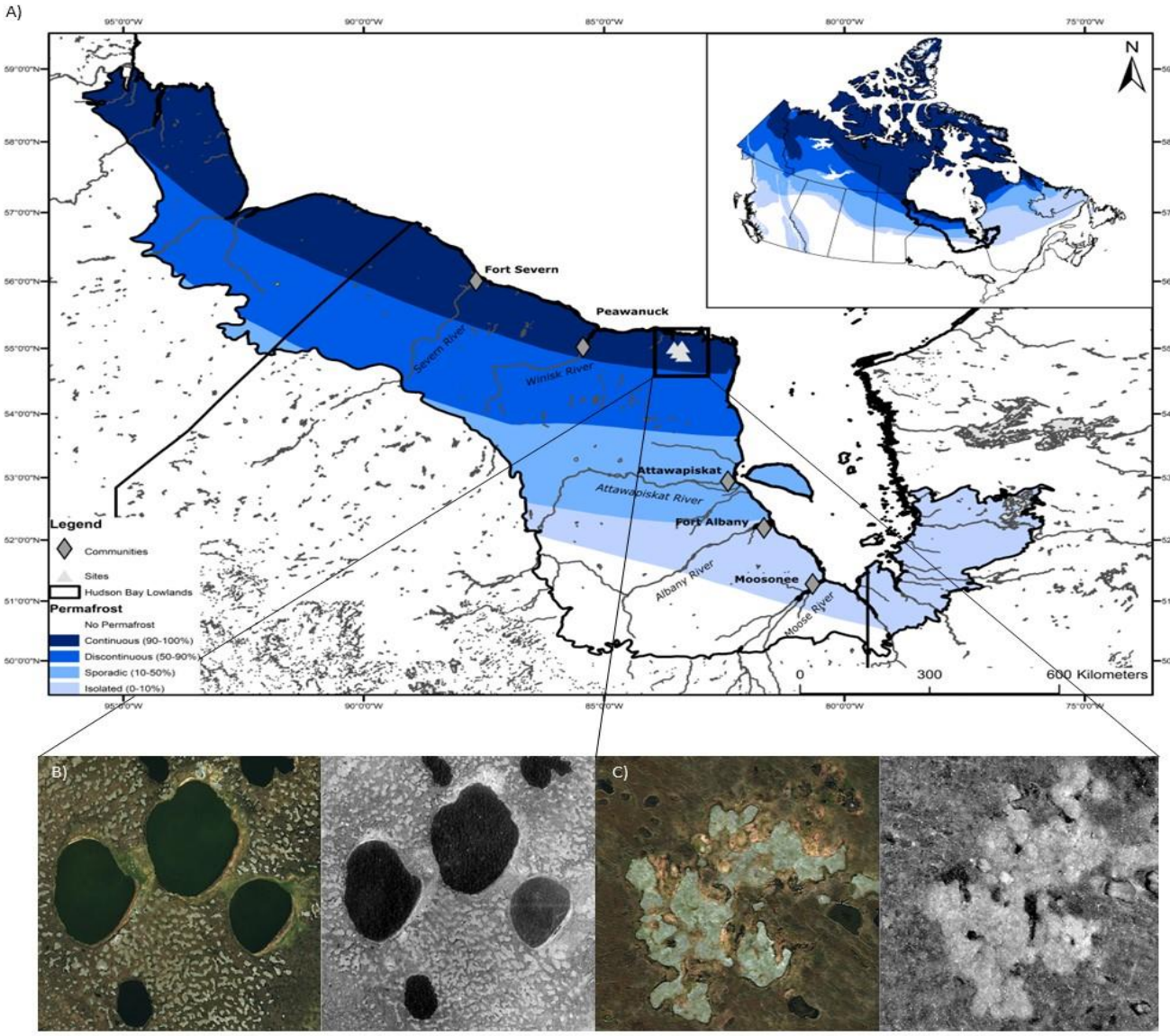

Figure 1: Map of the Hudson Bay Lowlands including study sites. The inset on A) shows Canadian permafrost distribution, with the HBL outlines in black. Inset B) shows recent (2018) satellite imagery (Bing Images) compared to historical air photos taken in 1955 of sites likely affected by active layer deepening, but not thermokarst encroachment. Inset C) shows the degradation of a palsa via thermokarst encroachment from recent (2018) satellite imagery (Bing Images) compared to historical air photo from 1955.

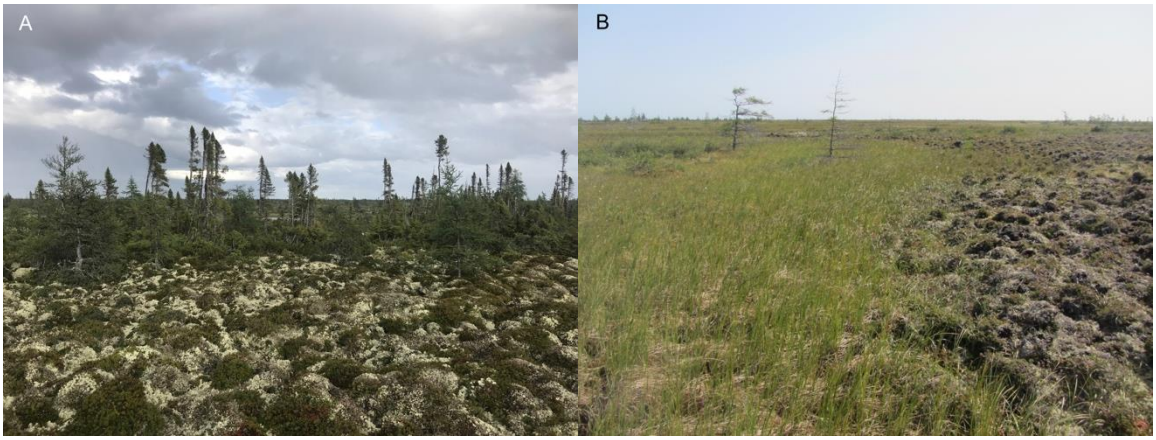

Figure 2: Typical vegetation found (A)on palsas including lichens, ericaceous shrubs, dwarf willow, and tamarack and spruce trees in the background, and (B) in thermokarst fens, dominated by graminoid such as *Carex spp.*

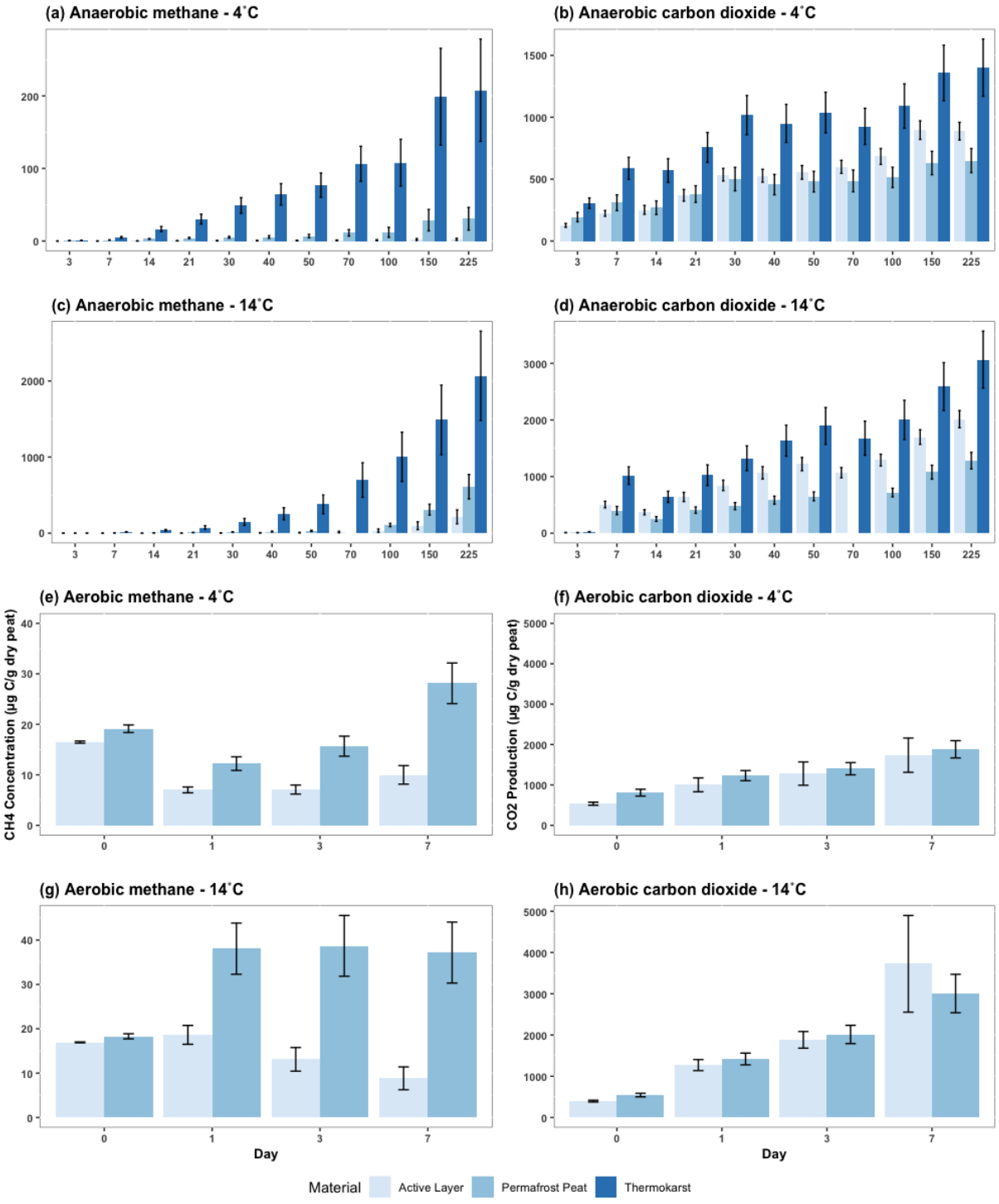

Figure 3: Production and consumption of CH_4 (left) and CO_2 (right) for anaerobic conditions over 225 days, and field moisture conditions over a period of 7 days. Error bars represent ± 1 standard error.

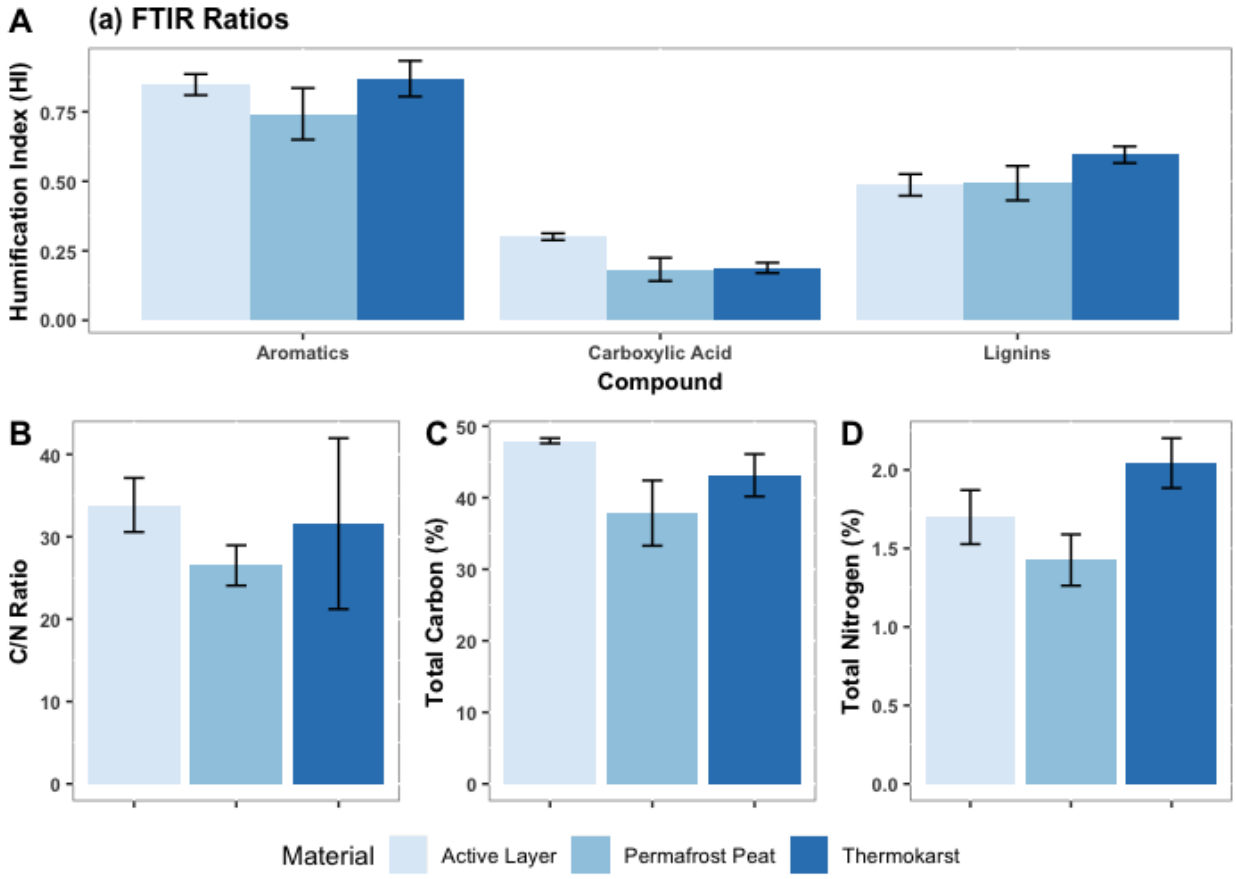

Figure 4: Carbon chemistry data as shown by Fourier-Transform Infrared (FTIR) spectroscopy (A) separated by material types for active layer, permafrost, and thermokarst peats. B-D shows elemental analysis for C:N ratio, Total C, and Total N, respectively, with error bars representing ± 1 standard error.

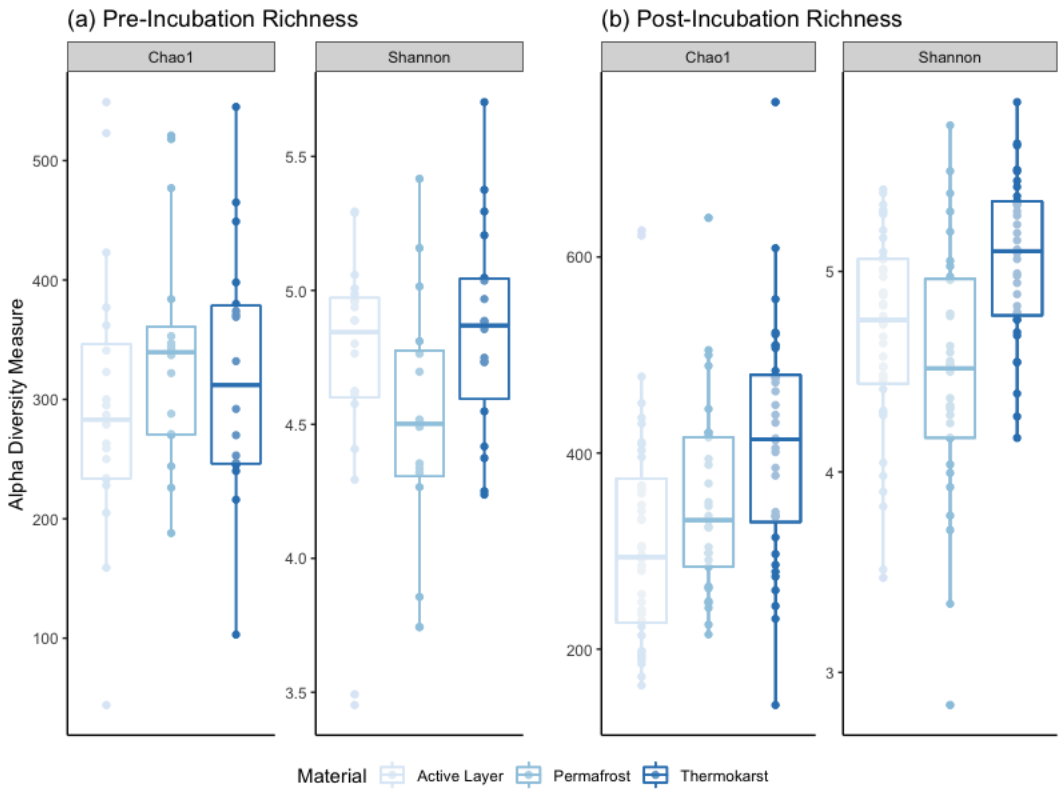

Figure 5: Alpha diversity of 16s rRNA communities pre-incubation (A) and post-incubation (B). Chao1 diversity is an estimation of microbial diversity based on abundance of species present, and Shannon diversity is an estimation based on both the abundance of species present as well as the evenness of species present.

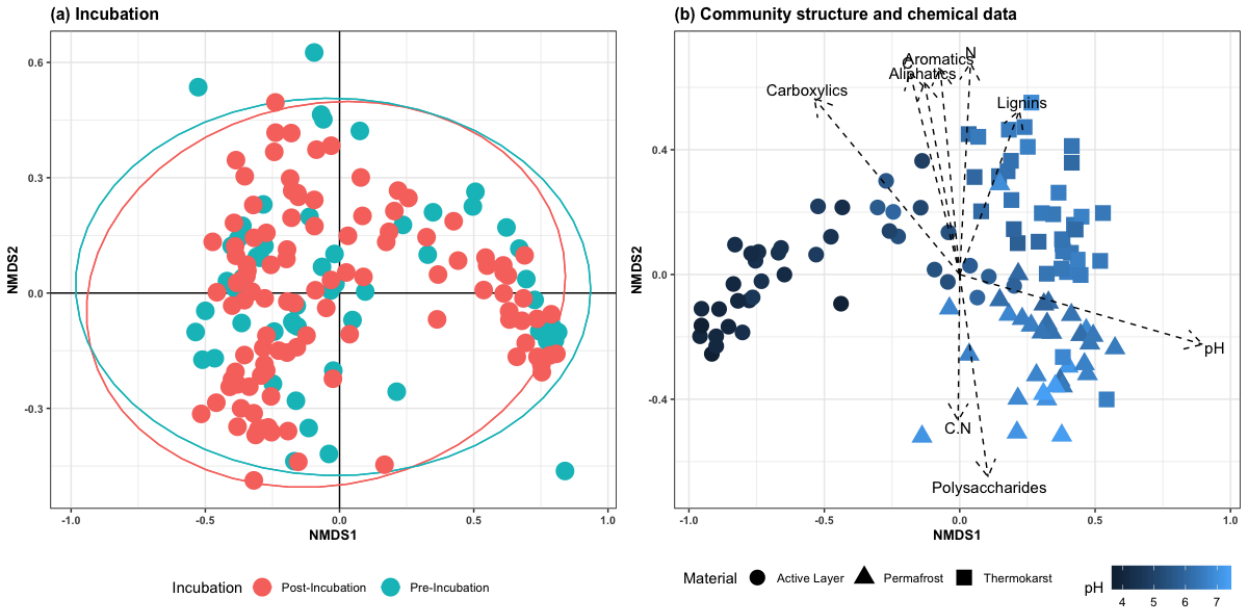

Figure 6: Nonmetric multidimensional scaling ordination of (a) microbial communities pre and post incubation, (b) and of post-incubation microbial communities where shape is peat type incubated, and colour is pH of the sample after 225 days of incubation. Arrows represent the effect of chemical properties from Fourier Transform Infrared (FTIR) Spectroscopy, total C (%) and N (%), ratio of C:N, and pH of the samples.

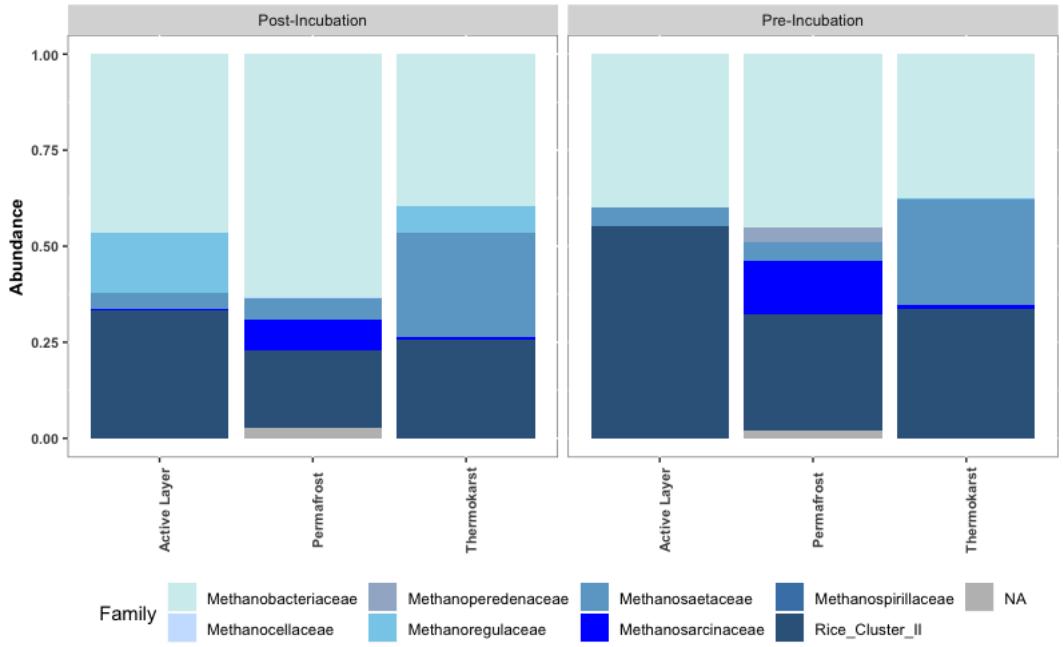

Figure 7: Methanogen communities as determined from 16s rRNA for post-incubation and pre-incubation. Communities were scaled to show relative abundance for total samples. Samples of each material were averaged to provide an overall estimate of methanogen structure for active layer, permafrost, and thermokarst peats.

8. Appendix: Supplementary Information

Supplementary Table 1: Correlation matrix (Pearson's product moment correlation) of Chao1 and Shannon diversity indices comparing diversity of microbial communities in each sample to the related greenhouse gas production and chemical compounds at 4˚C.

	Chao1		**Shannon**	
	r	p	r	p
CH4	0.10	0.323	**0.28**	**0.007**
CO2	0.02	0.877	**0.29**	**0.005**
Polysaccharides	-0.03	0.796	**-0.29**	**0.005**
Carboxylics	**-0.29**	**0.004**	0.01	0.889
Lignins	**0.26**	**0.013**	**0.38**	**<0.001**
Aromatics	0.04	0.676	**0.32**	**0.002**
N	0.18	0.088	**0.43**	**<0.001**
C	-0.06	0.568	**0.23**	**0.024**
C.N	-0.13	0.229	**-0.24**	**0.020**
pH	**0.38**	**<0.001**	0.17	0.101
S	0.18	0.082	**0.32**	**0.001**
Ca	0.12	0.249	-0.15	0.156
K	0.04	0.712	-0.20	0.059
Mg	0.03	0.762	**-0.25**	**0.017**
P	-0.15	0.154	-0.08	0.464

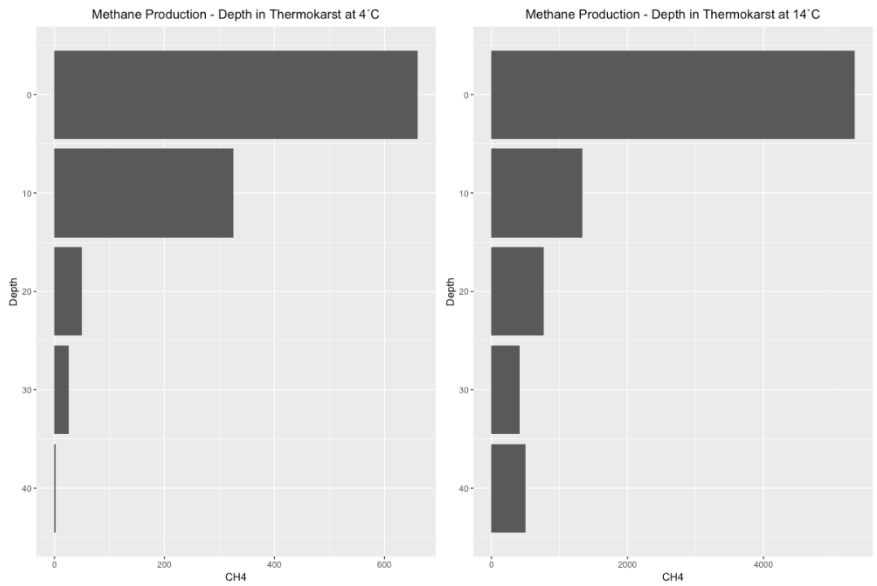

Supplementary Figure 1: CH_4 production by depth in thermokarst at 4˚C (left) and 14˚C (right). CH_4 concentrations measured in µg C/g dry peat.

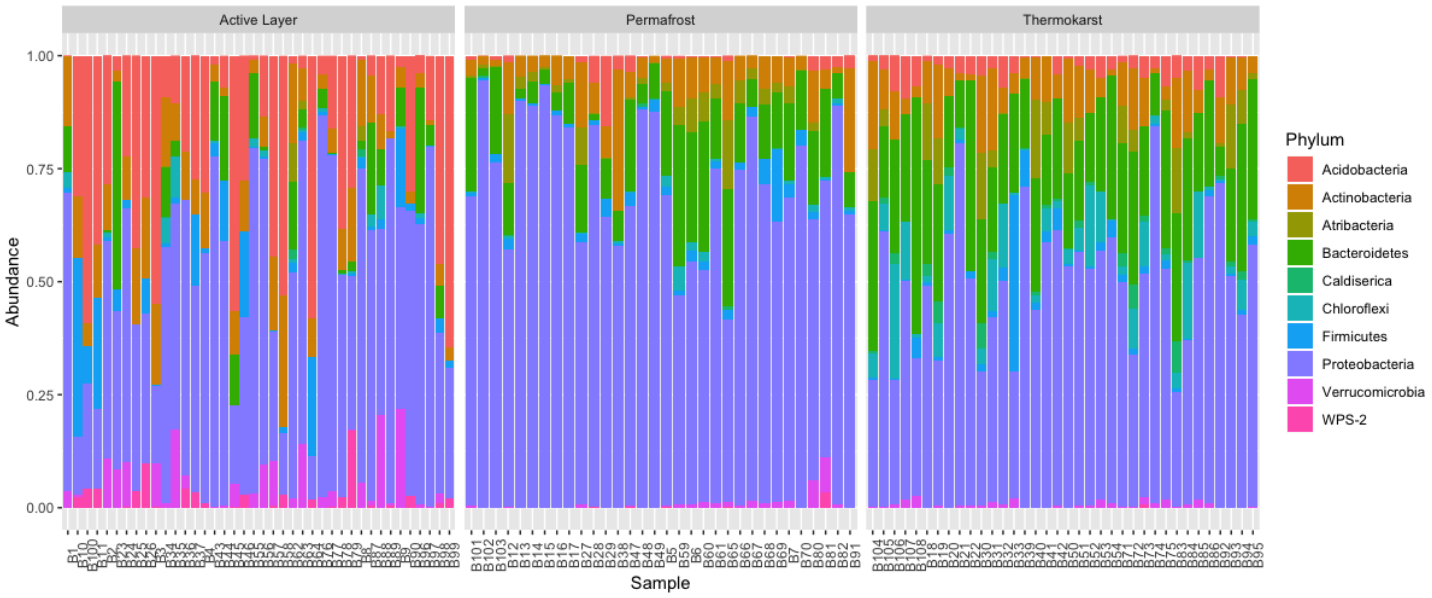

Supplementary Figure 2: Dominant phyla in active layer, permafrost, and thermokarst samples